

## Hollow fiber membrane reactors for the oxidative activation of ethane

Haihui Wang<sup>a,\*</sup>, Cristina Tablet<sup>a</sup>, Thomas Schiestel<sup>b</sup>, Jürgen Caro<sup>a</sup>

<sup>a</sup> *Institute of Physical Chemistry and Electrochemistry, University of Hanover, Callinstr. 3-3A, D-30167 Hanover, Germany*

<sup>b</sup> *Fraunhofer Institute for Interfacial Engineering and Biotechnology (IGB), Nobelstr. 12, D-70569 Stuttgart, Germany*

Available online 11 July 2006

### Abstract

A dense perovskite hollow fiber membrane made of the composition  $\text{BaCo}_x\text{Fe}_y\text{Zr}_z\text{O}_{3-\delta}$  (BCFZ,  $x + y + z = 1$ ) was fabricated by a phase inversion spinning followed by sintering. The oxygen permeation was investigated by operating with minor mass transfer resistance and oxygen partial pressure on the shell side and the core side of the hollow fiber membrane which can be adjusted by varying the air flow rates on the shell side (25–300 mL/min) and He flow rates on the core side (25–150 mL/min). A co-feed reactor and a periodically operated fixed-bed reactor were employed to estimate the BCFZ catalytic activity for the oxidative dehydrogenation of ethane to ethylene (ODE). Broken pieces of BCFZ pellets used in a packed bed reactor show that this perovskite possesses a moderate catalytic activity for the ODE at low temperature. For the first time the ODE was investigated in a hollow fiber membrane reactor made of the BCFZ. The best ethylene selectivity is about 64% which is lower than the 79% obtained in the BCFZ disk-shaped membrane. The reason is that the contact time on the two membrane configurations is different and the deeper oxidation of ethylene/ethane to CO and  $\text{CO}_2$  cannot be avoided in the hollow fiber membrane reactor.

© 2006 Elsevier B.V. All rights reserved.

**Keywords:** Perovskite; Oxidative dehydrogenation; Catalytic membrane reactor; Mixed conductor; Fibers

### 1. Introduction

The chemical industry depends heavily on ethylene as a chemical feedstock. Hence, there is a very strong incentive to study methodologies for the conversion of ethane to ethylene. Ethylene is currently produced by the thermal cracking of ethane, ethane–propane mixture, or naphtha [1], which is a highly endothermic and energy consumption intensive process with extensive coke formation. To overcome these problems, oxidation activation of alkanes such as the oxidative dehydrogenation of ethane to ethylene (ODE) is considered as an attractive alternative to the current thermal steam cracking process [2–5]. In addition to the fall away of any thermodynamic limitation of the conversion, lower operating temperatures and less coke formation are expected. Unfortunately, the yields attained so far in conventional co-feed reactors still remain too low for industrial application, because ethane reaction with oxygen results in the thermodynamically favored formation of

carbon oxides. In order to increase the selectivity for ethylene at a given conversion, a controlling of the contact mode of reactants is necessary. Dense mixed oxygen ion and electron conducting membranes offer a beneficial contact medium for the ODE. The advantage of the dense ceramic membrane reactor is that oxygen (air) is not co-fed with ethane, which avoids the formation of carbon oxides due to direct reactions between ethane and oxygen, thus higher ethylene selectivities can be expected. Previously we reported the ODE using planar and tubular oxygen permeable mixed ion and electron conducting membranes made of  $\text{Ba}_{0.5}\text{Sr}_{0.5}\text{Co}_{0.8}\text{Fe}_{0.2}\text{O}_{3-\delta}$  (BSCF) [6,7]. The ethylene selectivity of 80% for an ethane conversion of 84% was achieved at 800 °C. Rebeilleau et al. [8,9] also investigated the ODE in the BSCF catalytic membrane reactor. At 807 °C, an ethylene yield of 66% was obtained in the membrane reactor. After Pd cluster deposition, the ethylene yield reached 76% at 777 °C. However, Ni cluster deposition led to a decrease of ethane conversion compared to the bare membrane without changing ethylene selectivity. Akin and Lin found that per pass an ethylene yield of 56% with an ethylene selectivity of 80% was achieved in a dense tubular ceramic membrane reactor made of  $\text{Bi}_{1.5}\text{Y}_{0.3}\text{SmO}_3$  (BYS) at 875 °C [10].

\* Corresponding author. Tel.: +49 511 7622125; fax: +49 511 76219121.

E-mail address: [Haihui.Wang@pci.uni-hannover.de](mailto:Haihui.Wang@pci.uni-hannover.de) (H. Wang).

Recently, a novel perovskite hollow fiber membrane of the composition  $\text{BaCo}_x\text{Fe}_y\text{Zr}_z\text{O}_{3-\delta}$  (BCFZ,  $x + y + z = 1$ ) has been developed [11,12]. Compared with other configurations, hollow fiber membranes possess much larger membrane area per unit volume for oxygen permeation and can solve the problem of the high temperature sealing by adopting a long hollow fiber and keeping the two sealing ends away from the high temperature zone. The first results of the ODE in the BCFZ perovskite hollow fiber membrane reactor as well as the oxygen permeation behavior are presented in this paper.

## 2. Experimental

The BCFZ hollow fiber membrane was fabricated by a phase inversion spinning followed by sintering. A homogeneous slurry of a polymer solution and the BCFZ powder was obtained by ball milling up to 24 h with a solid content of 50–60 mass%. The slurry was spun through a spinneret and the obtained infinite green hollow fiber was cut into 0.5 m long pieces before sintering the fibers in a hanging geometry. During the calcination above 1300 °C the length and diameter of the green fiber reduced from 50 cm in length and 1 mm in diameter to ~30 cm in length and around ~0.80 mm in the outer diameter.

The hollow fiber membrane is cold-sealed with silicon seals at the ends, which were outside the hot zone of the oven, as shown in Fig. 1. The total length of the fiber is 30 cm and the oven length is 24 cm. Sixteen centimetres were regarded as effective fibre length at a temperature >500 °C (from the temperature profile of the 24 cm long oven). The effective surface area of the hollow fiber (3.52 cm<sup>2</sup>) was calculated based on 16 cm length because this material has no oxygen permeability when the temperature is lower than 500 °C. Since there is a temperature profile along the fiber, the oxygen permeation fluxes reported here are not accurate. More precise oxygen permeation fluxes were obtained using short fibers with Au paste as the high temperature sealing which can be found in our previous publication [12].

For the estimation of the non-reactive oxygen permeation flux, on the shell side air was used as the feed with a flow rate from 25 to 300 mL/min. Pure He (99.995%) flowed on the core side of the membrane at a flow rate varying from 25 to 150 mL/min. The gas flow rates were controlled by mass flow controllers (Bronkhorst). The gases at the exit of the permeator

were analyzed by a gas chromatograph (GC-Agilent 6890) equipped with the Carboxen 1000 column (Supelco). The oxygen permeation flux  $J_{\text{O}_2}$  (mL/cm<sup>2</sup> min) was calculated from the total flow rate  $V$  (mL/min) and the oxygen concentration of the exit gas  $\text{CO}_2$  (%) and the effective surface area of the membrane  $S$  (cm<sup>2</sup>) based on the following equation:

$$J_{\text{O}_2} = \frac{V \times C_{\text{O}_2}}{S} \quad (1)$$

For the ODE, ethane diluted with helium was fed to the core side, while air was fed to the shell side, as shown in Fig. 1. The products were analyzed by an online gas chromatograph (GC-Agilent 6890 equipped two auto valves) with Carboxen 1000 column (Supelco) which was used to separate  $\text{C}_2\text{H}_6$ ,  $\text{C}_2\text{H}_4$ ,  $\text{CH}_4$ ,  $\text{CO}$ ,  $\text{CO}_2$ ,  $\text{H}_2$ ,  $\text{N}_2$  and  $\text{O}_2$ . Concentrations of these species were determined by calibrating against the standard gases of all the product species. The quantity of  $\text{H}_2\text{O}$  was accounted for based on the hydrogen atom balance. The oxygen permeation flux was calculated from oxygen atoms of all the oxygen-containing products. The conversion of  $\text{C}_2\text{H}_6$ , selectivities of  $\text{C}_2\text{H}_4$ ,  $\text{CH}_4$ ,  $\text{CO}_2$ ,  $\text{CO}$  and the oxygen permeation flux in the ODE were defined as follows:

$\text{C}_2\text{H}_6$  conversion

$$= \frac{(1/2)F_{\text{CO}_2} + (1/2)F_{\text{CO}} + (1/2)F_{\text{CH}_4} + F_{\text{C}_2\text{H}_4}}{F_{\text{C}_2\text{H}_6}^{\text{feed}}} \quad (2)$$

$\text{C}_2\text{H}_4$  selectivity

$$= \frac{F_{\text{C}_2\text{H}_4}}{(1/2)F_{\text{CO}_2} + (1/2)F_{\text{CO}} + (1/2)F_{\text{CH}_4} + F_{\text{C}_2\text{H}_4}} \quad (3)$$

$\text{CH}_4$  selectivity

$$= \frac{(1/2)F_{\text{CH}_4}}{(1/2)F_{\text{CO}_2} + (1/2)F_{\text{CO}} + (1/2)F_{\text{CH}_4} + F_{\text{C}_2\text{H}_4}} \quad (4)$$

$\text{CO}$  selectivity

$$= \frac{(1/2)F_{\text{CO}}}{(1/2)F_{\text{CO}_2} + (1/2)F_{\text{CO}} + (1/2)F_{\text{CH}_4} + F_{\text{C}_2\text{H}_4}} \quad (5)$$

$\text{CO}_2$  selectivity

$$= \frac{(1/2)F_{\text{CO}_2}}{(1/2)F_{\text{CO}_2} + (1/2)F_{\text{CO}} + (1/2)F_{\text{CH}_4} + F_{\text{C}_2\text{H}_4}} \quad (6)$$

$$F_{\text{O}_2} = \frac{F_{\text{CO}} + F_{\text{H}_2\text{O}}}{2} + F_{\text{CO}_2} \quad (7)$$

$$J_{\text{O}_2} = \frac{F_{\text{O}_2}}{S} \quad (9)$$

where  $F_i$  is the flow rate of species  $i$  in mL/min, the membrane surface area  $S$  is 3.52 cm<sup>2</sup> in this study.

## 3. Results

Although the principle of the catalytic membrane reactor for the ODE is easily understood, in practice the concept is much more complex. Three aspects of membrane reactors and their

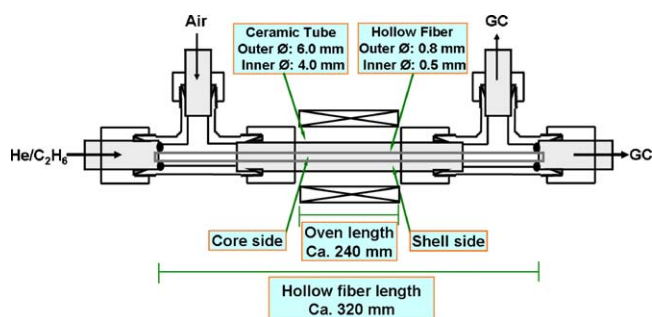


Fig. 1. Schematic diagram of the hollow fiber membrane reactor for oxygen permeation and the ODE.

relationship to each other have to be taken into account: (1) oxygen permeation rates through the hollow fiber with respect to the feed gas and sweep gas; (2) the intrinsic catalytic activity for the ODE of the membrane material; (3) the process parameters, which have a huge effect on the ODE performance and thus determine the ethane conversion, and ethylene selectivity. The relationships between the reaction rate, the flow rate, and the permeation rate through the hollow fiber membrane are very important in optimizing the process conditions.

### 3.1. Evaluation of the oxygen permeation through the BCFZ hollow fiber

Fig. 2 shows the influence of the air flow rate on the oxygen permeation flux through the hollow fiber membrane under different temperatures while the helium flow rate as the sweep gas on the core side was kept constant at 75 mL/min. The oxygen permeation flux increased with raising air flow rate until the air flow rate was higher than 250 mL/min. Further increase of the air flow rate led to no further increase of the oxygen permeation flux, as shown in Fig. 2. These results demonstrate that the external mass transport of oxygen to the membrane surface is the limiting step for the oxygen permeation if the flow rate of air is lower than 250 mL/min. A similar phenomenon was found in our previous study on the partial oxidation of methane to syngas (POM) in the BSCF oxygen permeable membrane reactor [13]. In order to eliminate the effect of air flow rate on the oxygen permeation flux, we have chosen a constant air flow rate of 300 mL/min in the following studies.

Fig. 3 shows the oxygen permeation flux as a function of the He flow rate on the core side. During this experiment the He flow rates were varied from 25 to 150 mL/min and the air flow rate was kept constant at 300 mL/min. A sharp increase of the oxygen permeation flux was observed when the He flow rate increased from 25 to 100 mL/min. However, the increase of the oxygen permeation flux becomes slow if the He flow rate on the core side is higher than 100 mL/min. The oxygen concentration

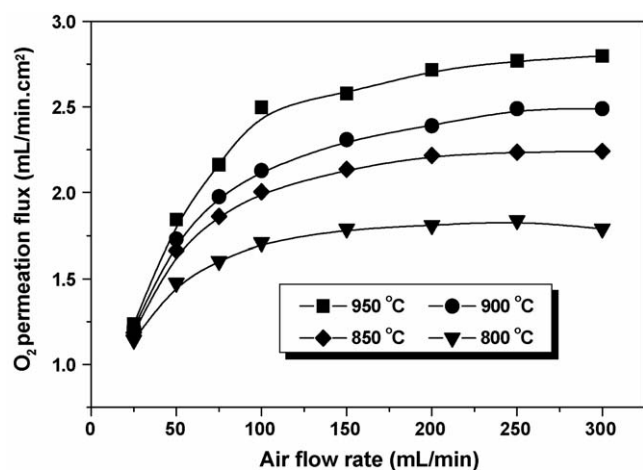


Fig. 2. Oxygen permeation flux through BCFZ hollow fiber as a function of air flow rates on the shell side. Membrane surface area: 3.52 cm<sup>2</sup>; He flow rate on the core side: 75 mL/min.

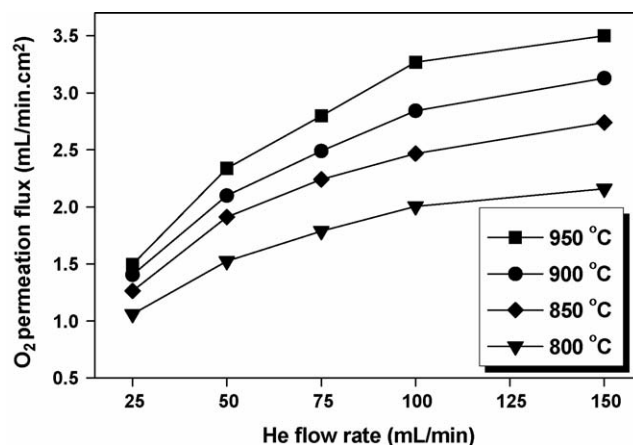


Fig. 3. Oxygen permeation flux through BCFZ hollow fiber membrane as a function of He flow rates on the core side. Membrane surface area: 3.52 cm<sup>2</sup>; air flow rate on the shell side: 300 mL/min.

on the core side decreases with increasing the sweep gas flow rate which leads to the increase of the driving force (Fig. 4), and thus a higher oxygen permeation flux is obtained for a higher He flow rate.

### 3.2. Test of the catalytic activity of BCFZ in the ODE

For a catalytic membrane reactor, the membrane material should not only possess sufficient oxygen permeability but also necessary catalytic activity for the ODE. Therefore, the catalytic activity of BCFZ for the ODE was investigated using pelletized BCFZ powder in a co-feed packed bed reactor. A quartz tube ( $\varnothing$  6 mm) was employed as the reactor. 0.6 g 30–60 meshes BCFZ particles were packed in the quartz reactor as the catalyst. Ethane and air were co-fed to the reactor. The mole ratio of ethane to air is 2:5, i.e. the mole ratio of ethane to oxygen is 2:1, which is the stoichiometric ratio of the ODE. The total flow rate of ethane and air is 40 mL/min. All the oxygen was consumed in the ODE. Ethane conversion and ethylene

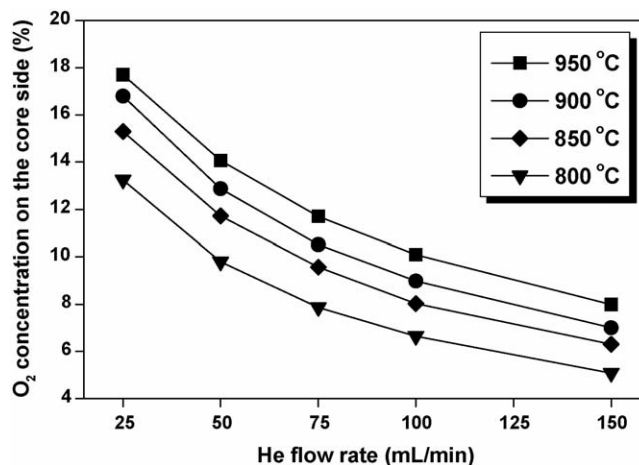


Fig. 4. Oxygen concentration on the core side as a function of He flow rates. Membrane surface area: 3.52 cm<sup>2</sup>; air flow rate on the shell side: 300 mL/min.

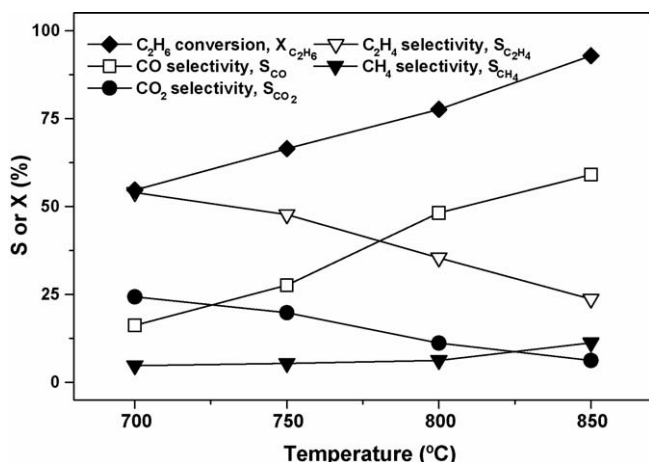


Fig. 5. Catalytic activity of BCFZ for the oxidative dehydrogenation of ethane to ethylene in a co-feed packed bed reactor with pelletized BCFZ powder as catalyst.

selectivity as a function of temperature are shown in Fig. 5. When the reaction temperature increased from 700 to 850 °C, ethane conversion increases from 55.0% to 98% and ethylene selectivity decreases from 54% to 24%. With increasing temperature, CO becomes the main product. These results demonstrate that the BCFZ shows moderate catalytic activity in the ODE reaction at lower temperatures.

The BCFZ catalytic activity of the ODE under a reducing environment was also tested in a quartz reactor (Ø 6 mm) with 0.6 g 30–60 meshes BCFZ particles under the periodically operated mode. Air was introduced to oxidize the BCFZ for 30 min, then helium instead of air swept the reactor until no nitrogen was detected; finally, a mixture of 10% ethane and 90% helium with the flow rate of 40 mL/min was introduced into the reactor. At 700 °C, the ethylene selectivity remained unchanged at around 88%, although the ethane conversion is low (~3%) and decreases with time. Compared with a reducing environment, lower ethylene selectivity was achieved in the present of O<sub>2</sub> in the

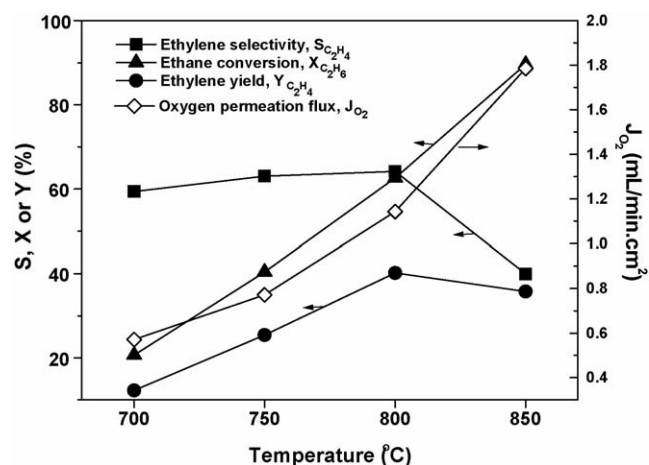


Fig. 6. The effect of temperature on the ethane conversion and product selectivity of ODE in the BCFZ hollow fiber membrane reactor. Feed: 40 mL/min a mixture of 10% ethane and 90% He on the core side; air flow rate on the shell side: 300 mL/min.

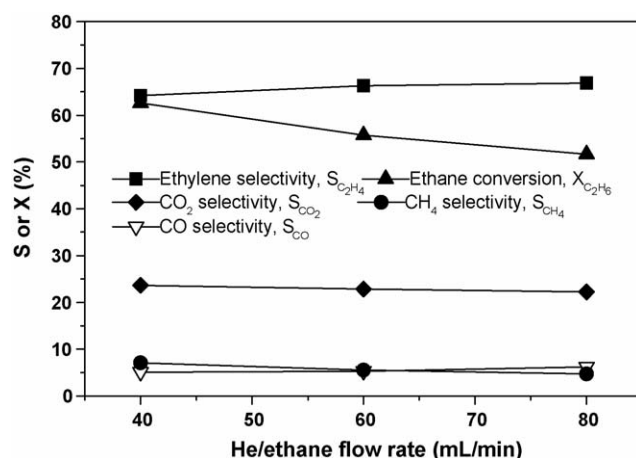


Fig. 7. The effect of flow rate of a mixture of 90% He diluted ethane on the ethane conversion and product selectivity of ODE in the BCFZ hollow fiber membrane reactor at 800 °C. Membrane surface area: 3.52 cm<sup>2</sup>; air flow rate on the shell side: 300 mL/min.

co-feed packed bed reactor, which was due to the reaction between the gaseous oxygen and the produced ethylene.

### 3.3. Membrane supported ODE

In order to avoid the gaseous oxygen contacting directly with ethane, the BCFZ membrane was employed as the reactor for the ODE. In this way, the ethane and the oxygen were separately fed to the reactor, so the ethylene selectivity could be increased. Furthermore, the oxygen can be continuously supplied through the membrane in the form of oxygen ions, so greater ethane conversion can be expected as was demonstrated in the previous papers using BSCF disk and tubular membrane reactors [6–9]. Fig. 6 shows the ethane conversion, the ethylene selectivity and the oxygen permeation flux as a function of temperature in the BCFZ hollow fiber membrane reactor. In this experiment, a mixture of 10% ethane and 90% helium was fed to the core side with the flow rate of 40 mL/min while air was fed to the shell side with the flow rate of 300 mL/min. It was found that the ethylene selectivity increases slightly from 59% to 64% and the ethane conversion increases from 21% to 63% when the temperature increases from 700 to 800 °C. Above 800 °C, however, the ethylene selectivity decreases sharply with increasing temperature.

Fig. 7 shows the effect of flow rate of a mixture of 90% He diluted ethane on the ethane conversion and product selectivities of the ODE in the BCFZ hollow fiber membrane reactor at 800 °C. The ethylene selectivity increases from 64% to 68% with increasing the total flow rate of He and ethane from 40 to 80 mL/min, i.e. decreasing the contact time from 0.078 to 0.039 s. This means that the contact time influences the ethylene selectivity; a shorter contact time gives higher ethylene selectivity.

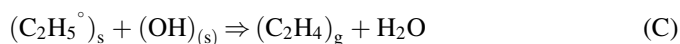
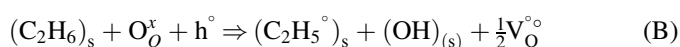
## 4. Discussion

At temperatures above 650 °C, the thermal dehydrogenation of ethane (TDE) to ethylene,  $C_2H_6 \rightleftharpoons C_2H_4 + H_2$ , is thermodynamically favored. Since our operation temperature is up to



850 °C, the ethane conversion through the TDE was of concern. However, the ethane conversion is determined by the reaction kinetics and reactor conditions. Akin and Lin [10] had estimated the TDE at 850 °C with a residence time of 0.07–0.1 s would result in less than 0.2% ethane conversion based on the available kinetic data (reaction order and rate constant) and plug flow reactor model [14]. In our hollow fiber membrane reactor presented here, the residence time is changed from 0.04 to 0.1 s, thus the TDE is not significant in our experiments. Actually from the experimental finding, we have also found  $\leq 1$  vol.% hydrogen in the product gases. Therefore the TDE is not discussed in the following.

In the ODE in the membrane reactor, ethane first is adsorbed at the catalytically active membrane surface where it reacts with lattice oxygen to form ethyl radicals and their subsequent decomposition to ethylene as [15]



where  $\text{V}_\text{O}^\circ$  are oxygen vacancies and  $\text{h}^\circ$  is electron holes.

Since reactions (C) and (D) are a fast irreversible reaction, the ethylene production rate is determined by reactions (A) and (B). If the reaction (B) cannot consume all of the lattice oxygen ( $\text{O}_\text{O}^\times$ ) completely or the reaction rate of Reaction (B) is not fast enough to consume the lattice oxygen in time, the formation of gaseous oxygen can occur:



Therefore, the lattice oxygen ( $\text{O}_\text{O}^\times$ ) on the membrane surface exposed to ethane is competitively consumed by two reactions: the ethane activation (reaction (B)) and the recombination of oxygen ions (reaction (E)). As we know, both the rate of ethane activation (reaction (B)) and the recombination rate of lattice oxygen to oxygen molecules (reaction (E)) increase with increasing temperatures. Since the gaseous oxygen produced in reaction E could further react with ethylene or ethane to form  $\text{CO}_x$ , thus decreasing the ethylene selectivity. So the ethylene selectivity is determined by the competition between reactions B and E. As shown in Fig. 6, the ethylene selectivity increased with raising the temperature when it is lower than 800 °C. However, when the temperature is higher than 800 °C, the ethylene selectivity decreased with increasing temperature. This result indicates that the recombination rate of lattice oxygen (reaction (E)) increases faster than the ethane activation (reaction (B)) at temperatures higher than 800 °C.

It is worthy of note that the oxygen permeation flux through the hollow fiber membrane during the ODE increases from 0.6 to 1.8 mL/min  $\text{cm}^2$  when the temperatures increase from 700 to 850 °C and no gaseous oxygen was found downstream corresponding to a total consumption of oxygen across the hollow fiber membrane. However, the oxygen permeation flux

Table 1

Comparison between BCFZ disk membrane reactor and BCFZ hollow fiber membrane reactor at 850 °C

Reactor types	$\text{C}_2\text{H}_6$ conversion (%)	Product selectivity (%)			
		$\text{C}_2\text{H}_4$	$\text{CH}_4$	$\text{CO}$	$\text{CO}_2$
Disk membrane reactor	85.2	79.1	10.7	5.4	4.8
Hollow fiber membrane reactor	89.6	39.9	12.1	15.4	32.6

Membrane surface area of disk membrane and hollow fiber are 0.90 and 3.52  $\text{cm}^2$ . Feed: 40 mL/min 90% He diluted ethane on the core side, air flow rate on the shell side: 300 mL/min.

improved only slightly compared with that using pure helium as sweep gas. This finding is similar to the previous results of the ODE on disk and tubular membranes made of BSCF [6,7] but different from the results of the partial oxidation of methane to syngas (POM). The oxygen permeation flux through the membrane during the POM is 5–10 times larger of that using pure helium as sweep gas [13,16]. The reason is that the POM is so fast that the lattice oxygen ( $\text{O}_\text{O}^\times$ ) can be consumed by reaction with methane once methane reaches the surface of the membrane in the present of a POM catalyst. As a result, the oxygen partial pressure on the membrane surface decreased sharply to a very low value ( $10^{-17}$  Pa) and leads to a large enhancement of the oxygen permeation flux. From the comparison of the oxygen permeation flux in the ODE and POM, it follows that the ODE reaction rate is not fast enough to consume the lattice oxygen ( $\text{O}_\text{O}^\times$ ) so that it could be recombined to gaseous oxygen and released to gas phase.

As shown in Table 1, for the comparable ethane conversion, the ethylene selectivity in the disk membrane reactor is much higher than that in the hollow fiber membrane reactor. More  $\text{CO}_2$  was produced in the hollow fiber membrane reactor than in the disk membrane reactor. This means that the deeper oxidation of ethane/ethylene cannot be avoided in the hollow fiber membrane reactor. As shown in Fig. 8, in the disk membrane reactor, the ethane reacted with lattice oxygen to form ethylene, and then the produced ethylene can leave the

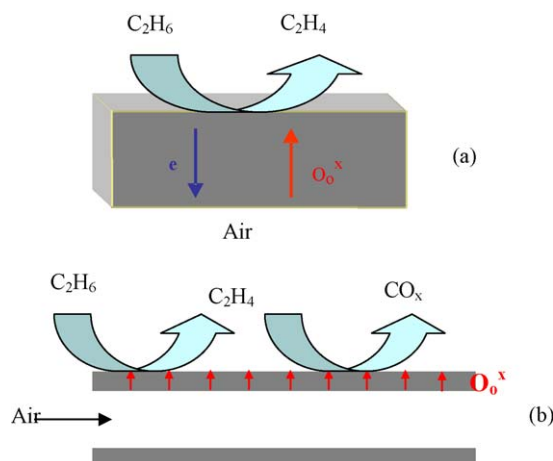


Fig. 8. The comparison of the ODE in the disk membrane reactor (a) and in the hollow fiber membrane reactor (b).

reactor in time. Therefore, the deep oxidation of ethylene can be largely avoided in the disk membrane reactor. However, for the hollow fiber membrane reactor, once ethylene was formed, it would react again with lattice oxygen or gaseous oxygen molecular to form  $\text{CO}_x$ . In the hollow fiber membrane reactor the contact time is 0.078 s, however, in the disk membrane reactor the contact time is 0.0023 s assuming 1 mm thickness above the membrane as the reaction zone. This means that the contact time in the disk membrane is much shorter than that in the hollow fiber reactor, which results in the higher ethylene selectivity in the disk membrane reactor.

Nevertheless the ODE in membrane reactors shows that a short contact time higher yields and selectivities than in classical packed bed reactors can be obtained in the co-feed operational mode. In general, for the oxidative dehydrogenation of light alkanes easily reducible oxide mixtures are used, a typical ethylene yield was ca. 30% on Mo–V–Nb oxides at relative low temperatures of 623–673 K [17]. During the last few years remarkable progress has been observed especially by reaction engineering optimization leading to ethylene yields of 56% at 71% selectivity in autothermal oxidative dehydrogenations at short contact times of ca. 45 ms using catalysts as ignitors [18]. Schmidt and co-workers [19,20] also used the concept of very short contact times on noble metal coated monoliths at 920 °C in the ms-range to get ethylene yields of 53–57% with selectivities from 66% to 70%. Comparing our best results on the disk shaped membrane (Table 1) where we can also realize short contact times, with the above data we can state that our ethylene yields of ca. 67% with selectivities of about 79% are higher than all data reported so far in the available literature. The selectivity found on our disk reactor is comparable with the selectivity obtained in the industrial ethylene production by thermal cracking but we have no thermodynamic limitation of the conversion.

## 5. Conclusion

In this paper, the oxygen permeation performance of the BCFZ hollow fiber membranes was investigated. Both the air flow rate on the shell side and the He flow rate on the core side have significant effects on the oxygen permeation flux of the hollow fiber. It was found that the external mass transport of oxygen on the membrane surface has an effect on the oxygen permeation when the flow rate of air is lower than 250 mL/min. The oxygen permeation flux was also found to increase with increasing helium flow rate because of the decreases of the oxygen concentration on the core side with increasing the sweep gas which leads to the increase of the driving force for the oxygen permeation.

The ODE catalytic activity of BCFZ was first tested both in the conventional co-feed packed bed reactor and the periodic shifted reactor, which shows that the BCFZ possesses moderate catalytic activity for ODE. The first results of the ODE using the BCFZ hollow fiber membrane are reported giving ethylene yields  $\leq 40\%$  at 800 °C. To get higher ethylene yields on the hollow fiber geometry, the reaction conditions of the ODE have to be optimized. Comparing the ODE using the BCFZ disk and hollow fiber membrane reactors, the ethylene selectivity on the disk membrane reactor was found to be  $\leq 80\%$  whereas using the hollow fiber membrane ethylene selectivity  $\leq 68\%$  was found. This experimental finding is explained by the different contact time on the two membrane configurations. Obviously, in the case of the hollow fiber membrane the deeper oxidation of ethylene to CO and  $\text{CO}_2$  could not be avoided.

## Acknowledgements

H. Wang expresses his thanks for the financial support from the Alexander von Humboldt Foundation. The perovskite fiber used was developed in the CaMeRa (Catalytic Membrane Reactor) project under the auspices of ConNeCat (Competence Network Catalysis) financed by the German Federal Ministry of Education and Research.

## References

- [1] L. Kniel, O. Winter, K. Stork, *Ethylene: Keystone to the Petrochemical Industry*, Dekker, New York, 1980.
- [2] H.H. Kung, *Adv. Catal.* 40 (1994) 1.
- [3] F. Cavani, F. Trifiro, *Catal. Today* 24 (1995) 307.
- [4] T. Blasco, J.M. Lopez Nieto, *Appl. Catal. A* 157 (1997) 117.
- [5] M. Banares, *Catal. Today* 51 (1999) 319.
- [6] H.H. Wang, Y. Cong, W.S. Yang, *Chem. Commun.* 14 (2002) 1468.
- [7] H.H. Wang, Y. Cong, W.S. Yang, *Catal. Lett.* 84 (2002) 101.
- [8] M. Rebeilleau, A.C. van Veen, D. Farrusseng, J. Rousset, C. Mirodatos, Z. Shao, G. Xiong, *Stud. Surf. Sci. Catal.* 147 (2004) 655.
- [9] M. Rebeilleau, S. Rosini, A.C. van Veen, D. Farrusseng, C. Mirodatos, *Catal. Today* 104 (2005) 131.
- [10] F.T. Akin, Y.S. Lin, *J. Membr. Sci.* 209 (2002) 457.
- [11] C. Tablet, G. Grubert, H.H. Wang, T. Schiestel, M. Schroeder, B. Langanke, J. Caro, *Catal. Today* 104 (2005) 126.
- [12] T. Schiestel, M. Kilgus, S. Peter, K.J. Caspary, H. Wang, J. Caro, *J. Membr. Sci.* 258 (2005) 1.
- [13] H.H. Wang, Y. Cong, W.S. Yang, *Catal. Today* 82 (2003) 157.
- [14] A.M. Brodsky, R.A. Kalienko, K.P. Lavrosky, *J. Chem. Soc.* 11 (1960) 4443.
- [15] J.H. Tong, W.S. Yang, R. Cai, B.C. Zhu, L. Lin, *Catal. Lett.* 78 (2002) 129.
- [16] S.A.R. Mulla, V.R. Choudhary, *J. Mol. Catal. A: Chem.* 223 (2004) 259.
- [17] M.E. Thorsteinson, T.P. Wilson, F.G. Young, P.H. Kasai, *J. Catal.* 52 (1978) 116.
- [18] S.A.R. Mulla, O.V. Buyevskaya, M. Baerns, *J. Catal.* 197 (2001) 43.
- [19] M. Huff, L.D. Schmidt, *J. Phys. Chem.* 97 (1993) 11815.
- [20] C. Yokoyama, S.S. Bharadwaj, L.D. Schmidt, *Catal. Lett.* 38 (1996) 181.